

Observation of internal-conversion electrons emitted from ^{229m}Th produced by β decay of ^{229}Ac Y. Shigekawa^{1,*}, Y. Kasamatsu,¹ E. Watanabe,¹ H. Ninomiya,¹ S. Hayami,¹ N. Kondo,¹
Y. Yasuda,¹ H. Haba,² and A. Shinohara¹¹Graduate School of Science, Osaka University, 1-1 Machikaneyama, Toyonaka, Osaka 560-0043, Japan²Nishina Center for Accelerator-Based Science, RIKEN, Wako, Saitama 351-0198, Japan

(Received 9 January 2019; revised manuscript received 13 June 2019; published 4 October 2019)

The first nuclear-excited state of ^{229}Th , ^{229m}Th , is known to have extremely low excitation energy at 8.28 ± 0.17 eV, and the nuclear decay mode and half-life of ^{229m}Th are considered to depend on its chemical environment. Recently, internal-conversion (IC) electrons from ^{229m}Th produced from a ^{233}U source were detected for the first time, and the half-life of ^{229m}Th on the nickel-alloy surface of a microchannel plate detector was determined. In this study, to determine the half-lives for other chemical environments, we produced ^{229m}Th through the β decay of ^{229}Ac and measured low-energy IC electrons from ^{229m}Th using the coincidence measurement technique between high-energy electrons (mainly β particles and high-energy IC electrons) and all electrons (including IC electrons from ^{229m}Th) emitted from an ^{229}Ac electrodeposited source. The ^{229}Ac nuclide was produced by the $^{232}\text{Th}(p, \alpha)^{229}\text{Ac}$ reaction and then was separated from a large amount of the reaction byproducts utilizing chemical separation techniques. Electron signals, which correspond to the IC electrons from ^{229m}Th , were detected using the coincidence measurement technique. The half-life of ^{229m}Th in the Ac electrodeposited source was determined to be $10(8) \mu\text{s}$, which is close to the previous experimental value. The method established in this study lays the foundations to study the IC-decay property of ^{229m}Th as a function of the chemical environment.

DOI: [10.1103/PhysRevC.100.044304](https://doi.org/10.1103/PhysRevC.100.044304)**I. INTRODUCTION**

The first nuclear-excited state of ^{229}Th (^{229m}Th) is known to have extremely low excitation energy at 8.28 ± 0.17 eV [1]. Because the excitation energy is close to the binding energy of valence electrons of the atomic Th, the nuclear decay mode (internal conversion, γ -ray emission, or electron bridge [2]) and half-life of ^{229m}Th are expected to vary depending on chemical environments [3,4]; thus, studying the decay property of the ^{229m}Th isomer should help us understand the interaction between the nucleus and valence electrons. Moreover, as the isomer energy is within reach of the current laser technology, the application of ^{229m}Th to the ultraprecise nuclear clock has recently been attracting much attention [5–7].

For studying the decay mode and half-life of ^{229m}Th for various chemical environments, it is important to directly detect the decay signals of ^{229m}Th (i.e., internal-conversion electrons, γ rays, and photons emitted through the electron bridge process [2]), but this approach was a challenge until now [8–16]. Recently, internal-conversion (IC) electrons from ^{229m}Th were detected for the first time [17], and the half-life was determined to be $7(1) \mu\text{s}$ when ^{229m}Th is on the nickel-alloy surface of a microchannel plate (MCP) detector [18]. These results are considered to be highly reliable because ^{229m}Th ions were transported a significant distance from a

highly radioactive ^{233}U source and other daughter products were removed with mass separation before measuring the IC electrons.

Half-life variations of a few nuclides such as ^{235m}U ($\approx 10\%$ [19–21]) and ^{99m}Tc ($\approx 0.3\%$ [22–24]) have been reported because the nuclei interact with outer-shell electrons in the IC process due to the low transition energies (76.7 eV for ^{235m}U [25] and 2.17 keV for ^{99m}Tc [26]). The half-life of ^{229m}Th (8.28 eV, comparable to chemical bond energy) that decays through the IC process is expected to vary; however, the half-life has so far been reported only for ^{229m}Th on the nickel-alloy surface environment [17]. Significantly different half-lives may be observed for other chemical environments such as $^{229m}\text{ThO}_2$ and $^{229m}\text{ThF}_4$ due to the extremely low excitation energy of ^{229m}Th . Such large half-life variation will help elucidate the chemical effects on the IC process. In this study, we propose a method to determine half-lives of ^{229m}Th for various chemical environments. In this method, ^{229m}Th is produced by β decay of ^{229}Ac . By measuring high-energy electrons (mainly β -particles and high energy IC electrons) and all electrons (including low-energy IC electrons from ^{229m}Th) emitted from a ^{229}Ac source in coincidence, the IC electrons from ^{229m}Th can be detected with several-microseconds delay from the emission of the high-energy electrons from ^{229}Ac . This approach has two advantages. First, the recoil energy of ^{229m}Th produced by the β decay of ^{229}Ac ($Q = 1104 \pm 12$ keV [27]) is less than 2.6 eV, which is lower than the dissociation energy of ionic and covalent bonds for most chemical environments. Therefore, it is considered that the chemical environment around ^{229m}Th

*Present address: Nishina Center for Accelerator-Based Science, RIKEN, Wako, Saitama 351-0198, Japan; yudai.shigekawa@riken.jp

would be almost the same as that around ^{229}Ac , and we can control the chemical composition of $^{229\text{m}}\text{Th}$ by controlling that of ^{229}Ac . For example, $^{229\text{m}}\text{Th}$ oxide can be prepared by electrodeposition of ^{229}Ac , and $^{229\text{m}}\text{Th}$ fluoride can be prepared by coprecipitating ^{229}Ac with ThF_4 [28]. Second, ^{229}Ac feeds $^{229\text{m}}\text{Th}$ with the branching ratio higher than 14%, due to the results of γ -ray spectroscopy of ^{229}Ac [29,30]. Such high branching ratio, compared with 2% when using a ^{233}U source [31,32], is a great advantage in the measurement of the IC electrons from $^{229\text{m}}\text{Th}$.

In spite of those advantages, it has been difficult to use ^{229}Ac for measuring the IC electrons from $^{229\text{m}}\text{Th}$ because ^{229}Ac can be produced only by accelerators and nuclear reactors and the half-life of ^{229}Ac is short (62.7 min [29,33]). A large amount of ^{229}Ac is required to compensate for the rapid decay of ^{229}Ac . The best method to acquire a large quantity of ^{229}Ac is a proton irradiation of ^{232}Th with an accelerator. This is because a large number of ^{232}Th atoms can be used as the target and the cross section for the $^{232}\text{Th}(p, \alpha)^{229}\text{Ac}$ reaction is relatively high (4.1 mb for the 20-MeV proton [34]). However, a large number of radioactive by-products (Th isotopes, Pa isotopes, and fission products) are produced by the proton irradiation. Therefore, chemical separation of ^{229}Ac must be conducted to directly detect the isomeric decay of $^{229\text{m}}\text{Th}$. The chemical purification of ^{229}Ac is challenging because it is difficult and time-consuming to remove lanthanides such as ^{142}La because they have similar chemical properties to ^{229}Ac . In this study, we succeeded in separating a sufficient amount of ^{229}Ac from a ^{232}Th target with a two-step sequence of cation exchange and extraction chromatography [35–37]. Then, we prepared an ^{229}Ac electrodeposited source and performed the coincidence measurement between high-energy electrons and all electrons for the ^{229}Ac source. We successfully observed signals corresponding to the IC electrons of $^{229\text{m}}\text{Th}$.

II. EXPERIMENT

^{229}Ac was produced by the $^{232}\text{Th}(p, \alpha)^{229}\text{Ac}$ reaction [34] at the Research Center for Nuclear Physics (RCNP), Osaka University. The ^{232}Th target (diameter 10 mm) was prepared by electrodepositing ^{232}Th on six pieces of Al foils (thickness 3 μm), and the total thickness of the ^{232}Th target was 6.5 mg/cm^2 . The proton beam energy and current were 20 MeV and about 2 μA , respectively. The irradiation time was 2 h.

The chemical separation was started after waiting for short-lived isotopes to decay out for about 1.5 h after the end of the proton beam irradiation period. The ^{232}Th target along with the Al backing foils was first dissolved with concentrated hydrochloric acid. After the solution was evaporated, the residue was dissolved with 2 ml of 1% citric acid (pH 2). The solution was fed onto a cation exchange column (Muromac 50WX8, 200–400 mesh, column volume ≈ 0.5 ml). ^{232}Th and most by-products such as ^{232}Pa , ^{105}Ru , and ^{97}Zr were eluted with 6 ml of 1% citric acid (pH 2) [35,36]. We poured 1 ml of 1 M nitric acid and then 5 ml of 6 M nitric acid into the column. Using a Ge detector, γ -ray spectra were measured for the ^{232}Th target, for the eluates of 1% citric

acid, 1 M nitric acid, and 6 M nitric acid, and for the column after separation. Because of high radioactivity of radioactive impurities, the γ -ray peaks for ^{229}Ac were not observed in these γ -ray spectra, and those for ^{228}Ac were observed only for the eluate of 6 M nitric acid. However, the yield of Ac isotopes in the cation exchange process can be estimated to be approximately 90%, judging from the yield of ^{142}La , chemical properties of which are very similar to Ac. In the eluate of 6 M nitric acid, the γ -ray peaks for ^{228}Ac , ^{91}Sr , ^{92}Sr , ^{139}Ba , ^{115}Cd , ^{117}Cd , ^{113}Ag , and lanthanides (e.g., ^{142}La and ^{143}Ce) were observed, and those isotopes were separated through a reversed-phase extraction chromatography using the Eichrom Ln resin. First, the eluate of 6 M nitric acid was evaporated, and the residue was dissolved with 1 ml of 0.05 M hydrochloric acid. Then, the solution was fed onto the Eichrom Ln resin (column volume ≈ 1.2 ml). Most of ^{92}Sr , ^{139}Ba , ^{115}Cd , ^{117}Cd , and ^{113}Ag were eluted with 6 ml of 0.05 M hydrochloric acid [37]. Subsequently, 10 ml of 0.1 M hydrochloric acid was poured into the column, and the eluates were collected in 0.5-ml fractions. A highly pure Ac solution, which did not include other elements, was obtained for 8th–10th fractions, judging from γ -ray spectroscopy using a Ge detector (see the result section for details). The total activity of ^{228}Ac in the 8th–10th fractions was $73 \pm 13\%$ of that in the eluate of 6 M nitric acid, meaning that the yield of Ac isotopes in the whole chemical separation process, including cation exchange and extraction chromatography, is about 60%. The whole chemical separation processes lasted approximately 4 h.

The ^{229}Ac source was prepared by electrodeposition [38] of ^{229}Ac on an 18- μm -thick Al foil per the following procedure. First, the 8th–10th fractions of the eluate of 0.1 M hydrochloric acid were mixed together and evaporated. Then, the residue was dissolved with the mixture of concentrated nitric acid and hydrogen peroxide water in order to reduce organic impurities. The solution was evaporated, and the residue was dissolved with 100 μl of 0.01 M nitric acid. 50 μl of the ^{229}Ac solution and 2.5 ml of 2-propanol were poured into an electrodeposition cell on the Al foil. We applied +400 V to a Pt anode soaked in the solution for 15 min. After the voltage was switched to 0 V, the Al foil with ^{229}Ac was heated at 150°C. The ^{229}Ac source preparation process lasted approximately 2 h. After γ -ray spectroscopy of the ^{229}Ac source, the source was placed in a vacuum chamber for coincidence measurement. The elapsed time from the end of the proton irradiation to the start of the coincidence measurement was 8.4 h. The γ -ray spectra of the ^{229}Ac source showed that the source included 99 ± 8 Bq of ^{229}Ac and 185 ± 9 Bq of ^{228}Ac at the start time of the coincidence measurement. The yield of the Ac isotopes in the electrodeposition process was found to be $15.1 \pm 0.9\%$.

The setup of the coincidence measurement between high-energy electrons and all electrons is depicted in Fig. 1. A plastic scintillator (diameter 10 mm, thickness 5 mm) and a Hamamatsu MPPC (multipixel photon counter) S13360-1350CS were placed below the ^{229}Ac source for the measurement of the high-energy electrons. High-energy electrons (more than ≈ 30 keV) could pass through the Al foil and were detected with the plastic scintillator. A two-stage MCP detector

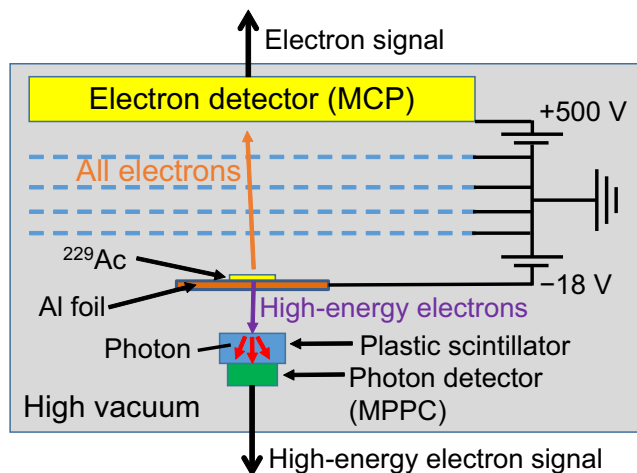


FIG. 1. Setup of the coincidence measurement between high-energy electrons (mainly β particles and high-energy IC electrons) and all electrons from ^{229}Ac . We applied -18 V to the ^{229}Ac source to push the low-energy IC electrons out of the surface, and $+500\text{ V}$ was applied to the surface of the MCP detector to maximize the detection efficiency for low energy electrons. The dashed lines between the ^{229}Ac source and the MCP detector represent metal meshes, which were kept grounded in this experiment.

(Hamamatsu F1942-04G, effective area of diameter 77 mm) was placed above the ^{229}Ac source for measuring all the electrons including low-energy IC electrons from $^{229\text{m}}\text{Th}$. The signals from both detectors were amplified with Ortec modules. The detection-time stamps of the signals corresponding to the high-energy electrons and all the electrons were registered with a time resolution of 500 ns, using the LIST mode of a 16-input PHA and LIST module (Niki Glass A3100). Based on the detection-time stamps of high-energy electrons and all electrons, time traces of all electrons following high-energy electrons were constructed.

III. RESULTS AND DISCUSSION

First, the purity of the Ac solution obtained through the chemical separation and the ^{229}Ac source obtained through the electrodeposition is shown. Fig. 2 shows the radioactivity of each isotope in each fraction of the eluate of 0.1 M hydrochloric acid, which was determined through γ -ray spectroscopy. The γ -ray peaks for ^{92}Sr , ^{139}Ba , ^{115}Cd , and ^{113}Ag were observed up to the 6th fraction, whereas only the peaks for ^{229}Ac and ^{228}Ac were observed for the 7th–10th fractions. The peaks for ^{142}La were observed from the 11th fraction. The sum of the radioactivity of non-Ac isotopes in the 8th–10th fractions should be much less than 0.1% of that of the Ac isotopes, considering the upper limit of radioactivity of each non-Ac isotope and the shapes of the elution curves. The γ -ray spectrum of the ^{229}Ac source prepared by electrodeposition using the 8th–10th fractions showed of course only the peaks for ^{229}Ac and ^{228}Ac , meaning that a highly pure Ac source was successfully prepared. Note that the γ -ray peaks for ^{226}Ac , which would be slightly produced through

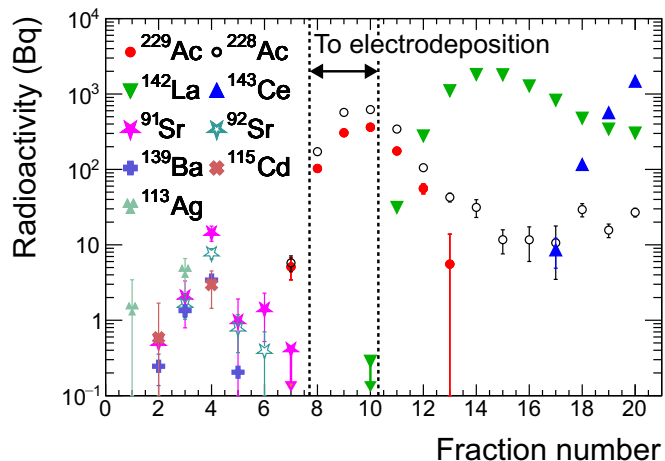


FIG. 2. Radioactivity of each isotope included in the eluates of 0.1 M hydrochloric acid as a function of the fraction number. The radioactivity of each isotope at the time of the γ -ray spectrum of each fraction having been measured is corrected to the radioactivity at the start time of the coincidence measurement (8.4 h after the end of the proton irradiation). The γ -ray peaks except for ^{229}Ac and ^{228}Ac were not observed in the 7th–10th fraction. The upper limit of radioactivity of ^{91}Sr in the 7th fraction and that of ^{142}La in the 10th fraction are shown for reference.

proton irradiation of ^{232}Th , were not observed in the γ -ray spectrum due to low radioactivity of ^{226}Ac .

Figure 3 shows the decay curve of the high-energy electrons detected with the plastic scintillator during the

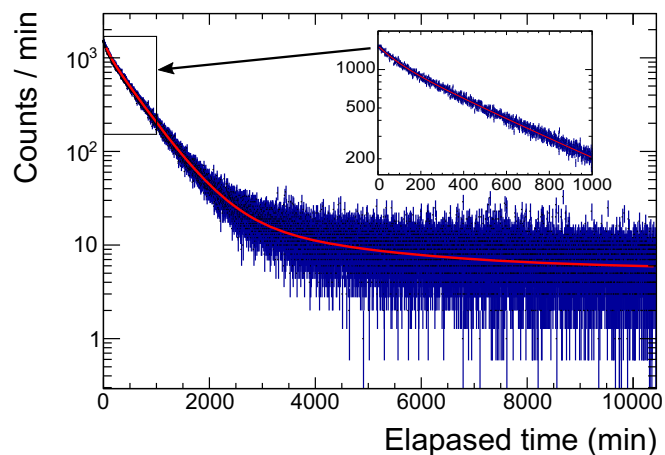


FIG. 3. Counts of the high-energy electrons (blue bar) as a function of the elapsed time from the start of the coincidence measurement. The sum of the exponential decay functions of ^{229}Ac ($T_{1/2} = 62.7\text{ min}$), ^{228}Ac ($T_{1/2} = 369.0\text{ min}$), and ^{226}Ac ($T_{1/2} = 1762.2\text{ min}$) plus a constant background was fitted to the data (red curve). Through fitting, count rates of the high-energy electrons from ^{229}Ac , ^{228}Ac , and ^{226}Ac at the start of the coincidence measurement were determined to be $302 \pm 7\text{ counts/min}$, $1197 \pm 2\text{ counts/min}$, and $24.0 \pm 0.3\text{ counts/min}$, respectively. The count rate of the constant background was determined to be $5.53 \pm 0.05\text{ counts/min}$.

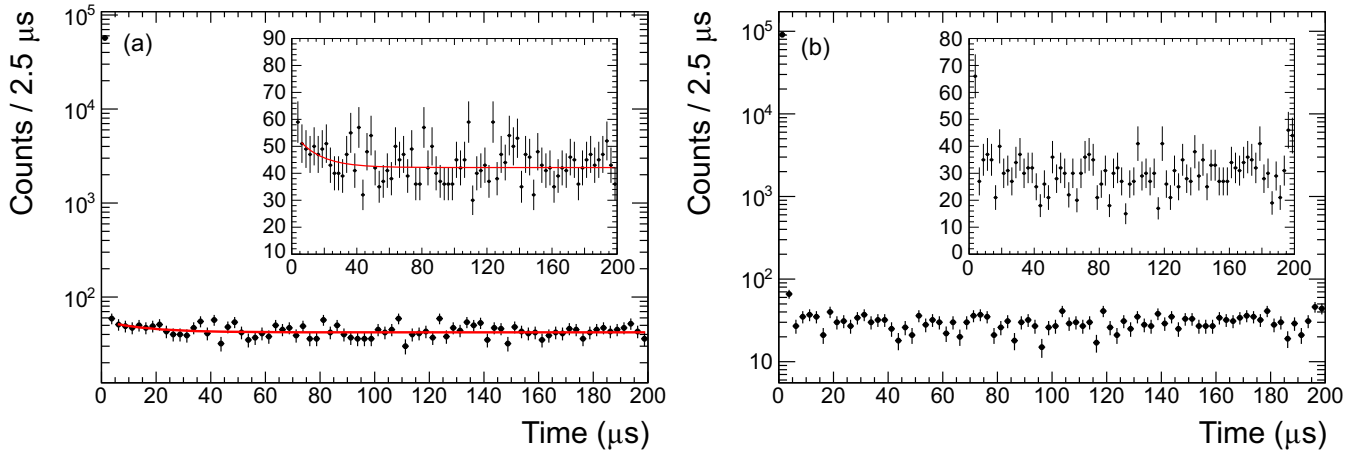


FIG. 4. Time traces of the all-electron signals triggered by the high-energy electron signals with the bins of $2.5 \mu\text{s}$ for (a) 0–120 min and (b) 300–800 min of the elapsed time from the start of the coincidence measurement. The same data are plotted on linear scales in the insets. The red line in graph (a) represents the fit curve of the exponential decay function plus a constant background.

coincidence measurement. The sum of the exponential decay functions of ^{229}Ac ($T_{1/2} = 62.7 \text{ min}$), ^{228}Ac ($T_{1/2} = 369.0 \text{ min}$), and ^{226}Ac ($T_{1/2} = 1762.2 \text{ min}$) plus a constant background (corresponding to the instrumental background) well reproduces the data. It was confirmed from the high-energy electron measurement that the actinium isotopes were successfully isolated from other radioactive elements as confirmed from the γ -ray spectroscopy.

Figure 4(a) shows the time trace of the all-electron signals (detected with the MCP detector) triggered by the high-energy electron signals (detected with the plastic scintillator) for 0–120 min of the elapsed time from the start of the coincidence measurement. Apparently, the counts in 0–25 μs exceed the constant background. In order to identify these excess counts, the time trace for 300–800 min of the elapsed time from the start of the coincidence measurement is shown in Fig. 4(b). In this elapsed time range, most ^{229}Ac decayed out, and the detected high-energy electrons predominantly originate from ^{228}Ac . Figure 4(b) shows that the counts in 0–5 μs exceed the constant background. The excess counts in the first 5 μs correspond to the prompt electrons that are produced just after the decay of ^{228}Ac . Because the half-lives of the nuclear excited states of ^{228}Th are less than 1 ns [39], all of the high-energy IC electrons emitted after the decay of ^{228}Ac should be counted in the bin of 0–2.5 μs . Hence, the counts in 2.5–5 μs should originate from atomic and chemical processes induced by the decay of ^{228}Ac , not from nuclear processes. For Fig. 4(a), including the decay of ^{229}Ac , all of the high-energy IC electrons emitted after the decay of ^{229}Ac should be counted in the bin of 0–2.5 μs because the half-lives of the nuclear excited states of ^{229}Th except for $^{229\text{m}}\text{Th}$ are less than 1 ns [33]. Therefore, the counts in 2.5–5 μs in Fig. 4(a) should originate from atomic and chemical processes, as the counts in 2.5–5 μs in Fig. 4(b), considering that atomic and chemical processes induced by the decay of ^{229}Ac should be very similar to those induced by the decay of ^{228}Ac . Consequently, the excess counts in 0–5 μs in Fig. 4(a) can be explained by the counts originating from prompt electrons, as the counts in 0–5 μs in Fig. 4(b). However, the

excess counts in 5–25 μs in Fig. 4(a) cannot be explained by prompt-electron counts and background counts, meaning that the counts in 5–25 μs correspond to the IC electrons of $^{229\text{m}}\text{Th}$. By fitting a single exponential decay function plus a constant background to the data in Fig. 4(a), the half-life of $^{229\text{m}}\text{Th}$ in the electrodeposition source ($^{229\text{m}}\text{Th}$ oxide or hydroxide) is determined to be 10(8) μs , which is comparable with that of $^{229\text{m}}\text{Th}$ on the nickel-alloy surface (7(1) μs [18]). Unfortunately, the half-life variation of $^{229\text{m}}\text{Th}$ depending on chemical environments was not clearly observed in this measurement because of the large error. However, we were able to confirm, using a different method than the original study [17,18], that the IC-decay channel of $^{229\text{m}}\text{Th}$ is indeed present and that the half-life is approximately 10^{-5} s [3].

To ensure that the excess counts in Fig. 4(a) indeed correspond to the IC electrons from $^{229\text{m}}\text{Th}$, the origin of the background counts are considered and are compared with the excess counts in Fig. 4(a). First, the background counts are compared with the expected counts of the random coincidence between the high-energy electrons (detected with the plastic scintillator) and all the electrons (detected with the MCP detector). The expected counts of the random coincidence $C_r(T_1, T_2)$ for the elapsed-time range from T_1 to T_2 is expressed as

$$C_r(T_1, T_2) = \int_{T_1}^{T_2} R_H(T)R_A(T)\Delta t dT, \quad (1)$$

where $R_H(T)$ and $R_A(T)$ are the count rates of the high-energy electrons and all the electrons at the elapsed time T , respectively. Δt is the time window of coincidence. $R_H(T)$ and $R_A(T)$ are expressed as

$$R_H(T) = \epsilon_H a_{229} n_{H,229} e^{-\frac{\ln(2)}{T_{229}} T} + \epsilon_H a_{228} n_{H,228} e^{-\frac{\ln(2)}{T_{228}} T} + \epsilon_H a_{226} n_{H,226} e^{-\frac{\ln(2)}{T_{226}} T} + b_H, \quad (2)$$

$$R_A(T) = \epsilon_A a_{229} n_{A,229} e^{-\frac{\ln(2)}{T_{229}} T} (1 - \epsilon_H n_{H,229}) + \epsilon_A a_{228} n_{A,228} e^{-\frac{\ln(2)}{T_{228}} T} (1 - \epsilon_H n_{H,228}) + \epsilon_A a_{226} n_{A,226} e^{-\frac{\ln(2)}{T_{226}} T} (1 - \epsilon_H n_{H,226}) + b_A, \quad (3)$$

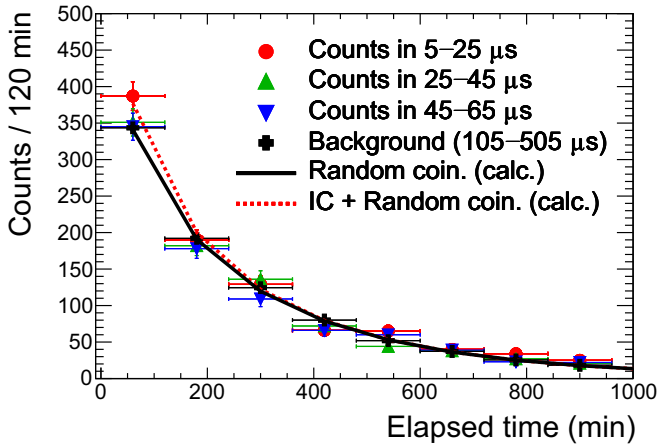


FIG. 5. Counts integrated over 5–25 μs (red circle), 25–45 μs (green triangle), 45–65 μs (blue inverted triangle) in the time traces of the all-electron signals [e.g. Fig. 4(a)] as a function of the elapsed time from the start of the coincidence measurement. The black cross plots represent the backgrounds that were obtained by averaging counts in 105–505 μs . The solid black line represents the calculated counts of random coincidence using Eqs. (1)–(3). The dashed red line represents the sum of the above-mentioned calculated counts of random coincidence and the IC-electron counts calculated by Eq. (4) on the assumption that $b\eta$ equals 4.2%.

respectively. T_{229} , T_{228} , and T_{226} are the half-lives of ^{229}Ac , ^{228}Ac , and ^{226}Ac , respectively. a_{229} , a_{228} , and a_{226} are the radioactivity of ^{229}Ac , ^{228}Ac , and ^{226}Ac at the start time of the coincidence measurement, respectively. $n_{H,229}$, $n_{H,228}$, and $n_{H,226}$ are the numbers of high-energy electrons emitted from the source per decay of ^{229}Ac , ^{228}Ac , and ^{226}Ac , respectively. $n_{A,229}$, $n_{A,228}$, and $n_{A,226}$ are the numbers of all electrons emitted from the source per decay of ^{229}Ac , ^{228}Ac , and ^{226}Ac , respectively. b_H and b_A are the background count rates of high-energy electrons and all electrons, respectively. ϵ_H and ϵ_A are the detection efficiency of high-energy electrons and all electrons, respectively. The correction factors $1 - \epsilon_H n_{H,229}$, $1 - \epsilon_H n_{H,228}$, and $1 - \epsilon_H n_{H,226}$ are introduced in Eq. (3) because an all-electron event that is detected in coincidence with a high-energy electron event must be a prompt and not a random event represented by Eq. (1). Note that b_A originates from the instrumental background of the MCP detector, and thus it was not multiplied by the correction factor. $\epsilon_H a_{229} n_{H,229}$, $\epsilon_H a_{228} n_{H,228}$, $\epsilon_H a_{226} n_{H,226}$, and b_H in Eq. (2) were determined to be 5.0 s^{-1} , 19.95 s^{-1} , 0.40 s^{-1} , and 0.092 s^{-1} , respectively, by the fitting shown in Fig. 3. $\epsilon_A a_{229} n_{A,229}$, $\epsilon_A a_{228} n_{A,228}$, $\epsilon_A a_{226} n_{A,226}$, and b_A in Eq. (3) were determined to be 21.2 s^{-1} , 108.5 s^{-1} , 2.5 s^{-1} , and 10.59 s^{-1} by fitting the decay curve of all-electron counts, as performed for high-energy electron counts in Fig. 3. $\epsilon_H n_{H,229}$ and $\epsilon_H n_{H,228}$ in Eq. (3) were determined to be 0.051 and 0.108 by dividing $\epsilon_H a_{229} n_{H,229}$ and $\epsilon_H a_{228} n_{H,228}$ by $a_{229} = 99 \text{ Bq}$ and $a_{228} = 185 \text{ Bq}$, respectively. $\epsilon_H n_{H,226}$ could not be precisely determined because a_{226} could not be determined from γ -ray spectroscopy. However, $\epsilon_H n_{H,226}$ could be estimated to be around 0.06 because the number of high-energy electrons ($>30 \text{ keV}$) emitted in the decay of ^{229}Ac , ^{228}Ac , and ^{226}Ac is

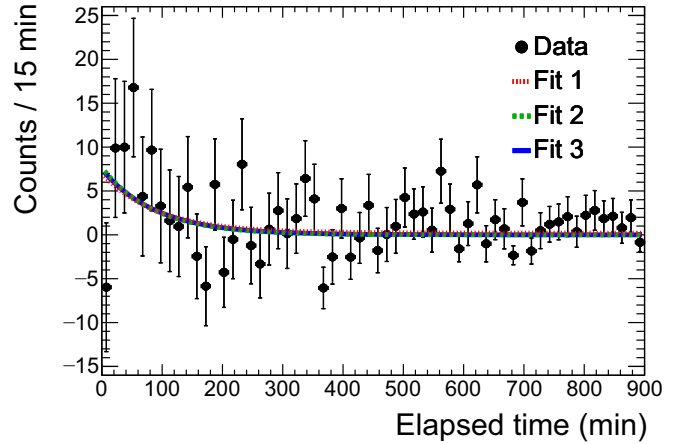


FIG. 6. Excess counts of electrons for 5–25 μs in the time traces of the all-electron signals as a function of the elapsed time from the start of the coincidence measurement with the bins of 15 min (closed circle). The excess counts of electrons were obtained by subtracting the counts of the backgrounds (average counts in 105–505 μs) from the counts integrated over 5–25 μs in the time traces of the all-electron signals. The three functions shown in the second column in Table I were fitted to the data (dotted red line, dashed green line, and solid blue line for Fit 1, Fit 2, and Fit 3, respectively).

1.06 [33], 1.93 [39], and 1.23 [40,41], respectively, and these values should be roughly proportional to $\epsilon_H n_{H,229}$, $\epsilon_H n_{H,228}$, and $\epsilon_H n_{H,226}$. By substituting $R_H(T)$ in Eq. (2), $R_A(T)$ in Eq. (3), and $\Delta t = 20 \mu\text{s}$ for Eq. (1), the random coincidence $C_r(T_1, T_2)$ for the 20- μs coincidence window as a function of the elapsed time was obtained as shown as the black line in Fig. 5. The background counts in the time traces [e.g., Fig. 4(a)] were obtained by averaging counts in 105–505 μs (black cross plots in Fig. 5). The calculated counts of random coincidence and the background counts of time traces are in good agreement with each other, meaning that the constant background counts in the time traces originate only from random coincidence. Next, the counts integrated over 5–25 μs , 25–45 μs , and 45–65 μs in the time traces for some elapsed time ranges are also shown in Fig. 5. It is found that only the counts in 5–25 μs for the elapsed-time range of 0–120 min exceed those of the background counts, while the counts in 5–25 μs for other elapsed-time ranges and those in 25–45 and 45–65 μs for all elapsed-time ranges are almost the same as those of the background counts. Hence, only the counts in 5–25 μs for the elapsed time 0–120 min cannot be explained by random coincidence. By subtracting the background counts (average counts in 105–505 μs) from counts in 5–25 μs , the excess-count dependence on the elapsed time was obtained as shown in Fig. 6. Three functions shown in Table I were fitted to the data in Fig. 6. Judging from the p values in the χ -square fittings, the three functions are relatively well fitted to the data. The result of the Fit 1 indicates that the counts originating from ^{228}Ac and ^{226}Ac are almost zero, meaning that the counts in Fig. 6 are originating only from ^{229}Ac . The Fit 2, where a single exponential function was fitted to the data without fixing the half-life, provided a half-life of $60 \pm 36 \text{ min}$, which is in good agreement with the half-life of ^{229}Ac

TABLE I. Functions fitted to the data in Fig. 6 (second column) and the results of the fittings (third column). T_{229} , T_{228} , and T_{226} in the second column are the half-lives of ^{229}Ac , ^{228}Ac , and ^{226}Ac , respectively. The resultant χ -square per degree of freedom and the p value for each χ -square fitting are shown in the fourth and fifth column, respectively.

Name	Fitted function	Result	χ^2/ndf	p value
Fit 1	$n_0 e^{-\frac{\ln(2)}{T_{229}} t}$	$n_0 = 6.8 \pm 4.3,$	1.06	0.36
	$+n_1 e^{-\frac{\ln(2)}{T_{228}} t}$	$n_1 = 0.0 \pm 2.1,$		
	$+n_2 e^{-\frac{\ln(2)}{T_{226}} t}$	$n_2 = 0.26 \pm 0.44$		
Fit 2	$n_0 e^{-\frac{\ln(2)}{T_{1/2}} t}$	$n_0 = 7.7 \pm 5.2,$ $T_{1/2} = 60 \pm 36 \text{ min}$	1.05	0.38
Fit 3	$n_0 e^{-\frac{\ln(2)}{T_{229}} t}$	$n_0 = 7.5 \pm 4.1$	1.03	0.42

($T_{1/2} = 62.7 \text{ min}$). Consequently, the counts in 5–25 μs , which exceed the counts of the background, are considered to originate from the decay of ^{229}Ac , not ^{228}Ac and ^{226}Ac , which supports the conclusion that the excess counts in 5–25 μs correspond to the IC electrons from $^{229\text{m}}\text{Th}$.

The number of excess counts in Fig. 6 is quantitatively discussed. The fitting of a single exponential decay function of ^{229}Ac to the data in Fig. 6 yielded 7.5 ± 4.1 counts / 15 min at the start of the coincidence measurement (Fit 3 in Table I), from which the total counts of the IC electrons detected in 5–25 μs are determined to be 49 ± 27 . The total IC-electron counts S in 5–25 μs can be calculated as

$$S = N_{H,229} b \eta \varepsilon_{e^-} (e^{-5/\tau} - e^{-25/\tau}), \quad (4)$$

where $N_{H,229}$ is the total number of detected high-energy electrons originating from ^{229}Ac , namely, $N_{H,229} = \int_0^\infty \epsilon_{HA229} n_{H,229} e^{-\frac{\ln(2)}{T_{229}} t} dt$. b is the branching ratio from ^{229}Ac to $^{229\text{m}}\text{Th}$, η is the escape efficiency, which indicates the probability that the IC electron of $^{229\text{m}}\text{Th}$ escapes from the solid surface, ε_{e^-} is the detection efficiency for electrons with several electronvolts, and τ is the lifetime of $^{229\text{m}}\text{Th}$ in microseconds. In this experiment, as $N_{H,229}$ equals $(2.73 \pm 0.06) \times 10^4$, ε_{e^-} is about 8%, and τ is 15(11) μs , $b\eta$ can be determined to be $4.2 \pm 3.4\%$. If the prepared source had no impurities, then the thickness of the source would be as thin as one atomic layer, and η would be close to 100%. However, the thickness of sources prepared by electrodeposition is usually larger than expected. The probable cause is the presence of organic compounds, originating from resin in ion chromatography and organic solvents in the electrodeposition. Assuming that the prepared ^{229}Ac source is made of only polystyrene, the thickness of it would be around 160 nm, which was obtained from the activity of ^{228}Th produced from ^{228}Ac and the number of ^{224}Ra (α -decay products of ^{228}Th) which escaped from the surface of the ^{229}Ac source [42]. Using the calculated mean free path of 10-eV electrons in polystyrene (21.7 nm [43]), η can be calculated as 6.8%, and thus b would be $62 \pm 49\%$, which is consistent with the fact that the branching ratio from ^{229}Ac to $^{229\text{m}}\text{Th}$ is higher than 14% [29,30]. Thus, the detected electron counts are

quantitatively consistent with the ones expected from Eq. (4), suggesting that the detected electrons would correspond to the IC electrons emitted from $^{229\text{m}}\text{Th}$. Note that this b value may be slightly different from the precise value as this calculation includes some assumptions.

In this study, we were able to detect the IC electrons emitted from $^{229\text{m}}\text{Th}$ in the Ac electrodeposited source. The method established here provides an independent verification of the IC decay of $^{229\text{m}}\text{Th}$ with an approximate half-life of 10^{-5} s [3,18], and lays the foundations for a future comparison of half-lives of $^{229\text{m}}\text{Th}$ for various well-controlled chemical environments such as ThO_2 , $\text{Th}(\text{OH})_4$, ThF_4 , and Th metal, by depositing ^{229}Ac into them. Moreover, the established method will also be the foundation for the IC-electron energy measurements from $^{229\text{m}}\text{Th}$ [1,44] for various chemical environments, which may lead to elucidating the nuclear-electron interaction in the IC process of $^{229\text{m}}\text{Th}$. To achieve this goal, the signal to background ratio needs to be improved, since in this experiment it was not high enough to precisely measure the half-life and the IC-electron energy. The background can be decreased by using a magnetic-bottle electron spectrometer [1,45–47], which would not allow high-energy electrons originating from the decay of ^{229}Ac and ^{228}Ac to reach an electron detector. The background may also be decreased by increasing the ^{229}Ac to ^{228}Ac ratio in the sample, which could be accomplished by making the chemical-separation time shorter. Moreover, the amount of ^{229}Ac available can be increased 100 times the amount achieved thus far by increasing the thickness of the ^{232}Th target and the proton-beam current. Consequently, the number of the counted IC electrons can be increased significantly. In the future, the suggested improvements to increase the signal to background ratio will enable precise measurement of the half-lives and the IC-electron energies for various chemical environments, which will lead to the elucidation of the IC-decay process of $^{229\text{m}}\text{Th}$.

IV. CONCLUSION

We produced ^{229}Ac by the $^{232}\text{Th}(p, \alpha)^{229}\text{Ac}$ reaction, and successfully separated ^{229}Ac from the ^{232}Th target and a large amount of by-products utilizing chemical separation techniques. Using the high-purity ^{229}Ac source prepared by electrodeposition, coincidence measurement between high-energy electrons and all electrons from ^{229}Ac was performed. Signals which correspond to the IC electrons of $^{229\text{m}}\text{Th}$ produced from ^{229}Ac were detected for the first time. The half-life of $^{229\text{m}}\text{Th}$ in the electrodeposition source was determined to be 10(8) μs , which is comparable with the previous experimental value for $^{229\text{m}}\text{Th}$ on a nickel-alloy surface [18]. The method established in this study lays the foundations to study the IC-decay of $^{229\text{m}}\text{Th}$ in various chemical environments.

ACKNOWLEDGMENTS

We are grateful to S. Stellmer, G. A. Kazakov, and T. Schumm for fruitful discussions. We also acknowledge the efforts of the operators in RCNP, Osaka University, for production of ^{229}Ac . This work was supported by JSPS Kakenhi Grants No. JP25800150 and No. JP16J06700.

- [1] B. Seiferle, L. von der Wense, P. V. Bilous, I. Amersdorffer, C. Lemell, F. Libisch, S. Stellmer, T. Schumm, C. E. Düllmann, A. Pálffy, and P. G. Thirolf, *Nature* **573**, 243 (2019).
- [2] V. F. Strizhov and E. V. Tkalya, *Sov. Phys. JETP* **72**, 387 (1991).
- [3] F. F. Karpeshin and M. B. Trzhaskovskaya, *Phys. Rev. C* **76**, 054313 (2007).
- [4] E. V. Tkalya, *Phys. Rev. Lett.* **120**, 122501 (2018).
- [5] E. Peik and C. Tamm, *Europhys. Lett.* **61**, 181 (2003).
- [6] C. J. Campbell, A. G. Radnaev, A. Kuzmich, V. A. Dzuba, V. V. Flambaum, and A. Derevianko, *Phys. Rev. Lett.* **108**, 120802 (2012).
- [7] G. A. Kazakov, A. N. Litvinov, V. I. Romanenko, L. P. Yatsenko, A. V. Romanenko, M. Schreitl, G. Winkler, and T. Schumm, *New J. Phys.* **14**, 083019 (2012).
- [8] S. B. Utter, P. Beiersdorfer, A. Barnes, R. W. Lougheed, J. R. Crespo López-Urrutia, J. A. Becker, and M. S. Weiss, *Phys. Rev. Lett.* **82**, 505 (1999).
- [9] E. Browne, E. B. Norman, R. D. Canaan, D. C. Glasgow, J. M. Keller, and J. P. Young, *Phys. Rev. C* **64**, 014311 (2001).
- [10] Y. Kasamatsu, H. Kikunaga, K. Takamiya, T. Mitsugashira, T. Nakanishi, Y. Ohkubo, T. Ohtsuki, W. Sato, and A. Shinohara, *Radiochim. Acta* **93**, 511 (2005).
- [11] E. Peik and K. Zimmermann, *Phys. Rev. Lett.* **111**, 018901 (2013).
- [12] A. Yamaguchi, M. Kolbe, H. Kaser, T. Reichel, A. Gottwald, and E. Peik, *New J. Phys.* **17**, 053053 (2015).
- [13] J. Jeet, C. Schneider, S. T. Sullivan, W. G. Rellergert, S. Mirzadeh, A. Cassanho, H. P. Jenssen, E. V. Tkalya, and E. R. Hudson, *Phys. Rev. Lett.* **114**, 253001 (2015).
- [14] E. L. Swanberg, Ph.D. thesis, University of California, Berkeley (2012).
- [15] K. Zimmermann, Ph.D. thesis, Univ. Hannover, Germany (2010).
- [16] S. Stellmer, Y. Shigekawa, V. Rosecker, G. A. Kazakov, Y. Kasamatsu, Y. Yasuda, A. Shinohara, and T. Schumm, *Phys. Rev. C* **98**, 014317 (2018).
- [17] L. von der Wense, B. Seiferle, M. Laatiaoui, J. B. Neumayr, H.-J. Maier, H.-F. Wirth, C. Mokry, J. Runke, K. Eberhardt, C. E. Düllmann, N. G. Trautmann, and P. G. Thirolf, *Nature* **533**, 47 (2016).
- [18] B. Seiferle, L. von der Wense, and P. G. Thirolf, *Phys. Rev. Lett.* **118**, 042501 (2017).
- [19] M. N. de Mévergnes, *Phys. Rev. Lett.* **29**, 1188 (1972).
- [20] M. N. de Mévergnes and P. Del Marmol, *Phys. Lett. B* **49**, 428 (1974).
- [21] Y. Shigekawa, Y. Kasamatsu, Y. Yasuda, M. Kaneko, M. Watanabe, and A. Shinohara, *Phys. Rev. C* **98**, 014306 (2018).
- [22] K. T. Bainbridge, M. Goldhaber, and E. Wilson, *Phys. Rev.* **84**, 1260 (1951).
- [23] K. T. Bainbridge, M. Goldhaber, and E. Wilson, *Phys. Rev.* **90**, 430 (1953).
- [24] H. Mazaki, S. Kakiuchi, T. Mukoyama, and M. Matsui, *Phys. Rev. C* **21**, 344 (1980).
- [25] F. Ponce, E. Swanberg, J. Burke, R. Henderson, and S. Friedrich, *Phys. Rev. C* **97**, 054310 (2018).
- [26] E. Browne and J. K. Tuli, *Nucl. Data Sheets* **145**, 25 (2017).
- [27] M. Wang, G. Audi, F. G. Kondev, W. J. Huang, S. Naimi, and X. Xu, *Chin. Phys. C* **41**, 030003 (2017).
- [28] T. Mitsugashira, M. Hara, P. Kim, K. Nakashima, and K. Nakayama, *J. Radioanal. Nucl. Chem.* **255**, 201 (2003).
- [29] K. Gulda, W. Kurcewicz, A. J. Aas, M. J. G. Borge, D. G. Burke, B. Fogelberg, I. S. Grant, E. Hagebø, N. Kaffrell, J. Kvasil, G. Løvholden, H. Mach, A. Mackova, T. Martinez, G. Nyman, B. Rubio, J. L. Tain, O. Tengblad, and T. F. Thorsteinsen, *Nucl. Phys. A* **703**, 45 (2002).
- [30] E. Ruchowska, W. A. Plóciennik, J. Żylicz, H. Mach, J. Kvasil, A. Algora, N. Amzal, T. Bäck, M. G. Borge, R. Boutami, P. A. Butler, J. Cederkäll, B. Cederwall, B. Fogelberg, L. M. Fraile, H. O. U. Fynbo, E. Hagebø, P. Hoff, H. Gausemel, A. Jungclaus, R. Kaczarowski, A. Kerek, W. Kurcewicz, K. Lagergren, E. Nacher, B. Rubio, A. Syntfeld, O. Tengblad, A. A. Wasilewski, and L. Weissman, *Phys. Rev. C* **73**, 044326 (2006).
- [31] V. Barci, G. Ardisson, G. Barci-Funel, B. Weiss, O. El Samad, and R. K. Sheline, *Phys. Rev. C* **68**, 034329 (2003).
- [32] J. Thielking, M. V. Okhapkin, P. Glowacki, D. M. Meier, L. von der Wense, B. Seiferle, C. E. Düllmann, P. G. Thirolf, and E. Peik, *Nature* **556**, 321 (2018).
- [33] E. Browne and J. K. Tuli, *Nucl. Data Sheets* **109**, 2657 (2008).
- [34] L. Milazzo-Colli, G. M. Braga-Marcazzan, and M. Milazzo, *Il Nuovo Cimento A* **30**, 632 (1975).
- [35] V. Radchenko, J. W. Engle, J. J. Wilson, J. R. Maassen, F. M. Nortier, W. A. Taylor, E. R. Birnbaum, L. A. Hudston, K. D. John, and M. E. Fassbender, *J. Chromatogr. A* **1380**, 55 (2015).
- [36] T. Mastren, V. Radchenko, A. Owens, R. Copping, R. Boll, J. R. Griswold, S. Mirzadeh, L. E. Wyant, M. Brugh, J. W. Engle, F. M. Nortier, E. R. Birnbaum, K. D. John, and M. E. Fassbender, *Sci. Rep.* **7**, 8216 (2017).
- [37] V. Ostapenko, A. Vasiliev, E. Lapshina, S. Ermolaev, R. Aliev, Yu. Totskiy, B. Zhuikov, and S. Kalmykov, *J. Radioanal. Nucl. Chem.* **306**, 707 (2015).
- [38] N. Trautmann and H. Folger, *Nucl. Instrum. Methods Phys. Res. Sect. Accel. Spectrometers Detect. Assoc. Equip.* **282**, 102 (1989).
- [39] K. Abusaleem, *Nucl. Data Sheets* **116**, 163 (2014).
- [40] Y. A. Akovali, *Nucl. Data Sheets* **77**, 433 (1996).
- [41] S. Singh, A. K. Jain, and J. K. Tuli, *Nucl. Data Sheets* **112**, 2851 (2011).
- [42] Y. Shigekawa, Y. Kasamatsu, and A. Shinohara, *Rev. Sci. Instrum.* **87**, 053508 (2016).
- [43] J. C. Ashley, C. J. Tung, and R. H. Ritchie, *IEEE Trans. Nucl. Sci.* **25**, 1566 (1978).
- [44] B. Seiferle, L. von der Wense, and P. G. Thirolf, *Eur. Phys. J. A* **53**, 108 (2017).
- [45] Y. Yamakita, H. Tanaka, R. Maruyama, H. Yamakado, F. Misaizu, and K. Ohno, *Rev. Sci. Instrum.* **71**, 3042 (2000).
- [46] P. Kruit and F. H. Read, *J. Phys. E: Sci. Instrum.* **16**, 313 (1983).
- [47] B. Seiferle, L. von der Wense, I. Amersdorffer, N. Arlt, B. Kotulski, and P. G. Thirolf, *Nucl. Instrum. Methods Phys. Res. Sect. B* (2019), doi:10.1016/j.nimb.2019.03.043.